Energy-Efficient Resource Management for Multi-UAV-Enabled Mobile Edge Computing

Yu Zhang, Student Member, IEEE, Yanmin Gong, Senior Member, IEEE, and Yuanxiong Guo, Senior Member, IEEE,

Abstract-Unmanned aerial vehicles (UAVs) have been widely utilized to expand wireless network coverage and provide computation service for Internet-of-Things (IoT) devices in signalblocked or shadowed environments. In this paper, we propose a novel multi-UAV-enabled mobile edge computing (MEC) architecture in which multiple UAVs provide both communication and computation services for IoT devices that cannot directly access the ground edge clouds. To achieve min-max fairness of energy consumption among UAVs, we minimize the maximal energy consumption among UAVs by jointly optimizing computation offloading decisions, communication and computation resource allocation, UAV positions, and task splitting decisions, while meeting the delay requirement of all tasks. The required optimization is a large-scale mixed-integer non-linear program that is generally intractable. To solve this problem, we propose an efficient iterative algorithm based on the successive convex approximation (SCA). The simulation results show that the proposed scheme outperforms various baseline schemes in processing computation-intensive and latency-critical tasks.

Index Terms—Mobile edge computing, successive convex approximation, unmanned aerial vehicle, resource management.

I. INTRODUCTION

S Internet-of-Things (IoT) devices are flourishing as never before, it is estimated that 79.4 zettabytes of data will be generated by 2025 [1]. These data will cause an enormous burden on traditional cloud computing networks. Besides, the emerging artificial intelligence applications of IoT devices, such as smart cities [2] and real-time video analytics [3], [4], are typically computation-intensive and latency-critical. It is challenging for traditional cloud computing systems to provide these services.

To meet the quality of service (QoS) requirement, mobile edge computing (MEC) is a promising approach. Unlike traditional cloud computing, which relies on remote cloud servers for task processing, MEC handles tasks on small cloud computing platforms (i.e., edge clouds) deployed at the network edge. By relocating communication and computation resources in proximity to IoT devices where data are generated, MEC can efficiently reduce network congestion, provide low-latency computation service, and boost network security [5]–[8]. Nevertheless, traditional terrestrial MEC is still infeasible in signal-blocked or shadowed environments

due to the immobility of infrastructure-based edge clouds (ECs).

In recent years, UAV-enabled wireless networks have gained increasing attention. By exploiting the high altitude and mobility of UAVs, these networks can efficiently provide line-ofsight (LoS) communication and real-time computation services for IoT devices that are beyond the coverage of infrastructurebased ECs. For instance, AT&T and Verizon have leveraged UAVs to provide temporarily boosted Internet coverage for Super Bowl and college football national championship [9]. There are two major challenges in UAV-enabled wireless networks. One challenge is how to deploy UAVs to ensure the quality of communication and computation services, while another is how to achieve fair computation offloading and resource allocation to reduce UAVs' energy consumption. There is a substantial literature to tackle these challenges. However, most existing works either investigate the UAVenabled wireless networks in terms of communication aspect while ignoring the computation capability provided by the UAVs [10]–[13], or they just consider a single UAV for computation offloading [14]–[17]. Recently, a few studies have tried to investigate a multi-UAV-enabled MEC system [18]-[24]. The multi-UAV-enabled MEC systems, where ground users offload their computation tasks to UAVs for processing, have been explored in [18], [19]. Furthermore, ongoing research is studying how multiple UAVs and a ground EC can collaborate to provide computational services to ground users, aiming to optimize system latency [20] or energy efficiency [21]. Besides, reinforcement learning is widely used to optimize system latency and energy consumption in MEC systems involving multiple UAVs and ground ECs [22]–[24]. However, managing a large number of UAVs, ground users, and ECs can lead to exponential growth in the states (e.g., UAV positions) and actions (e.g., computation offloading decisions) of reinforcement learning. This increase can significantly impair convergence efficiency. Moreover, it's important to note that the objectives of the aforementioned studies are minimizing energy consumption and/or task processing delay, overlooking the fairness of energy consumption among UAVs.

This paper investigates how to achieve the min-max fairness of energy consumption among UAVs in a novel multi-UAV-enabled MEC system. In this system, multiple UAVs provide both communication and computation services to ground IoT devices that can not access ground ECs directly. Specifically, each ground IoT device connects with a UAV and offloads its computation-intensive and latency-critical tasks to that UAV. Then, the UAV splits the tasks into two parts: one executed on

1

Y. Zhang and Y. Gong are with the Department of Electrical and Computer Engineering, University of Texas at San Antonio, San Antonio, Texas, 78249, USA. (e-mail: {yu.zhang@my., yanmin.gong@}utsa.edu).

Y. Guo is with the Department of Information Systems and Cyber Security, University of Texas at San Antonio, San Antonio, Texas, 78249, USA. (e-mail: yuanxiong.guo@utsa.edu).

the UAV and the other relayed to the more powerful computational ground ECs. We aim to minimize the maximal energy consumption among UAVs jointly optimizing computation offloading decisions, communication and computation resource allocation, UAV positions, and task splitting decisions, while meeting the delay requirement of all tasks. The problem is formulated as a mixed-integer non-linear program (MINLP), which is generally intractable. To solve this problem, we developed an efficient solution algorithm based on successive convex approximation (SCA). Particularly, we adopt auxiliary variables and convex approximation to transform the original non-convex objective function and constraints into sequential convex ones. By iteratively solving these approximated convex problems, we obtain a suboptimal solution for the original MINLP. The convergence of the proposed algorithm can be guaranteed by the properly designed diminishing step-size rule.

The main contributions of this paper are summarized as follows.

- We propose a cutting-edge multi-UAV-enabled MEC system where multiple UAVs and ground ECs cooperatively provide communication and computation services to the ground IoT devices.
- A joint optimization problem is formulated to minimize the maximal energy consumption among UAVs subject to the delay requirement.
- As the formulated problem is a MINLP, which is generally intractable, we reformulate it into a feasible one utilizing convex approximation. Then, we design an efficient SCA-based algorithm to obtain an approximate solution.
- We conduct extensive numerical experiments to evaluate the performance of our proposed scheme. Simulation results show the proposed scheme outperforms the baseline schemes, especially for processing computation-intensive and latency-crucial tasks.

The remainder of this paper is organized as follows. The related works are reviewed in Section II. The system model and problem formulation are described in Section III. In Section IV, we present the SCA-based algorithm to solve the formulated problem. Simulation results are presented in Section V. Finally, Section VI concludes this paper.

II. RELATED WORKS

UAVs have been receiving significant attention in wireless communication due to their mobility and high altitude. For instance, UAVs can act as aerial base stations, flying over designated areas to provide reliable downlink and uplink communication for ground users [10]–[13]. In the last decade, more and more studies have emphasized the computation capacity of UAVs [14]–[24]. However, most existing research has focused on the scenario of a single UAV for computation offloading [14]–[17]. Due to limited battery life and computation capacity, a single UAV may fall short of providing sufficient computation service for emerging artificial intelligence applications. Therefore, exploring a MEC system where multiple UAVs collaboratively provide computation services for ground users is a more suitable approach [18]–[24]. A multi-UAV-enabled MEC system usually consists of three entities, i.e,

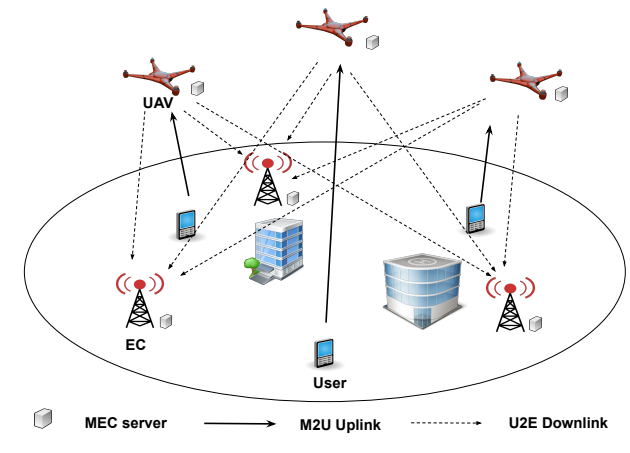


Fig. 1: The multi-UAV-enabled MEC system.

UAVs, ground users and base stations. The interactions of communication and computation between multiple UAVs and ground users have been analyzed in [18], [19], while the collaboration involving multiple UAVs, ground users, and a single base station has been explored in [20], [21]. Only a few recent studies consider a multi-UAV-enabled MEC system where multiple UAVs and ground ECs collaboratively provide the computation service for ground users. Based on game theory and reinforcement learning, Asheralieva et al. [22] studied a computation offloading and cooperation problem in a multi-UAV-enabled MEC system, where privately-owned UAVs are deployed as quasi-stationary base stations to cooperate with privately-owned ground base stations. Zhao et al. [23] formulated a joint trajectory designing, computation task offloading, and communication resource allocation problem with the goal of minimizing the sum of execution delay and energy consumption. Chen et al. [24] jointly optimized UAV trajectory, ground user association, and transmit power to minimize the weighted sum of the overall system latency and energy consumption.

However, multi-UAV-enabled MEC systems face new challenges. Typically, the operational cycle of these systems is constrained by the UAV with the shortest battery life. Hence, the fairness of energy consumption among UAVs is crucial to maintain the normal operation of the systems. Based on this motivation, we aim to minimize the maximal energy consumption among UAVs by jointly optimizing computation offloading decisions, communication and computation resource allocation, UAV positions, and task splitting decisions, while meeting the delay requirement of all tasks. To the best of our knowledge, this is the first paper to investigate the min-max fairness of energy consumption among UAVs for a multi-UAV-enabled MEC system involving multiple UAVs, ground ECs and IoT devices.

III. SYSTEM MODEL AND PROBLEM FORMULATION

As illustrated in Fig. 1, we consider a multi-UAV-enabled MEC system which consists of a set of UAVs $k \in \mathcal{K} = \{1,\ldots,K\}$, a set of ground ECs $j \in \mathcal{J} = \{1,\ldots,J\}$ and a set of ground IoT devices $i \in \mathcal{I} = \{1,\ldots,I\}$. The IoT devices are referred to as mobile users (MUs) in the rest of our

paper. The UAVs are deployed to assist the MUs by providing both communication and computation services. Specifically, each MU first offloads the computation tasks to the associated UAV. Then, the UAV processes a portion of the tasks locally and relays the remaining tasks to ECs, ensuring all tasks meet their delay requirements. In this wireless network setup, we consider a scenario where a network provider collects the state of the UAV network, which includes communication and computation resources, IoT device locations, and so on. Then, the provider executes the proposed algorithm to minimize the maximal energy consumption among UAVs. We focus on two major communications: MU-to-UAV (M2U) uplink communication and UAV-to-EC (U2E) downlink communication.

Without loss of generality, we assume each UAV is equipped with a limited computational edge server powered by its embedded batteries. On the other hand, the ground ECs, i.e., cellular base stations, are endowed with sufficient computation capabilities and are able to provide ultra-high-speed transmission rates with the grid power supply. Each MU i has ongoing time-intensive and computation-intensive tasks $G_i = (S_i, C_i, \xi_i)$, where S_i denotes the size of each input task, C_i represents the required CPU cycles for processing 1-bit of input task, and ξ_i indicates the task arrival rate. Besides, we assume that the input tasks are bit-wise independent and can be processed in a partial offloading fashion [25].

We denote the association between UAV k and MU i as $\beta_{i,k} \in \{0,1\}$. $\beta_{i,k} = 1$ indicates MU i is associated with UAV k; otherwise $\beta_{i,k} = 0$. Considering each MU i is associated with only one UAV, we have

$$\sum_{k \in \mathcal{K}} \beta_{i,k} = 1, \quad \forall i. \tag{1}$$

After establishing an association with MU i and completing the task transmission, UAV k will split the task into two parts: one part to be processed onboard, denoted as $\alpha_{i,k,0} \in [0,1]$, and the other to be relayed to ground EC j, denoted as $\alpha_{i,k,j} \in [0,1]$. This can be modeled as the following constraint:

$$\alpha_{i,k,0} + \sum_{i \in \mathcal{J}} \alpha_{i,k,j} = \beta_{i,k}, \quad \forall i, k.$$
 (2)

In this paper, we represent the locations of MUs, UAVs and ECs through the 3D Cartesian coordinate system. The locations of ground MU i and EC j are denoted as $\boldsymbol{Q}_i = (x_i, y_i, 0)$ and $\boldsymbol{Q}_j = (x_j, y_j, 0)$, respectively. According to [26]–[29], we assume the UAVs fly at a fixed height H and denote the location of UAV k as $\boldsymbol{q}_k = (x_k, y_k, H)$. To avoid collisions, the distance between any two UAVs must maintain a minimum distance L^{\min} . Thus, another constraint holds:

$$\|\boldsymbol{q}_{k'} - \boldsymbol{q}_k\|^2 \ge L^{\min}, \quad \forall k \ne k',$$
 (3)

where $\|\cdot\|$ denotes the Euclidean norm of a vector.

A. Communication Model

We consider both the large-scale and small-scale fadings for the M2U and U2E channels in this multi-UAV-enabled MEC network [30]. Hence, the channel gains of M2U and U2E can be defined by

$$h_{i,k} = \tilde{g}_{i,k}\tilde{h}_{i,k}$$

$$= \frac{h_0}{\|\mathbf{Q}_i - \mathbf{q}_k\|^2} \left(\sqrt{\frac{K}{K+1}} + \sqrt{\frac{1}{K+1}} g_{i,k} \right)^2, \quad (4)$$

$$h_{k,j} = \tilde{g}_{k,j}\tilde{h}_{k,j}$$

$$= \frac{h_0}{\|\mathbf{Q}_j - \mathbf{q}_k\|^2} \left(\sqrt{\frac{K}{K+1}} + \sqrt{\frac{1}{K+1}} g_{k,j} \right)^2, \quad (5)$$

respectively, where $\{\tilde{g}_{i,k}, \tilde{g}_{k,j}\}$ and $\{\tilde{h}_{i,k}, \tilde{h}_{k,j}\}$ are the large-scale and small-scale fading coefficients of M2U and U2E channels, respectively. h_0 is the channel gain at a reference distance of 1 meter [31], [32]. $\{g_{i,k}, g_{k,j}\} \in \mathcal{CN}(0,1)$ and K is the Rician factor that corresponds to the ratio between the LoS power and the scattering power 1 .

We assume the frequency division multiple access (FDMA) protocols are adopted in the M2U and U2E communications. Besides, channel overlapping and interference are not considered in our scenario. After establishing the association with MU i, UAV k will allocate $B_{i,k}^{\rm M2U}$ bandwidth for the communication. Since the sum of allocated bandwidth cannot exceed the total bandwidth of UAV k, we have the following constraint on $B_{i,k}^{\rm M2U}$:

$$\sum_{i \in \mathcal{I}} B_{i,k}^{\text{M2U}} \le B_k^{\text{M2U}}, \quad \forall k, \tag{6}$$

where $B_k^{\rm M2U}$ denotes the total M2U bandwidth of UAV k.

Based on Shannon's theorem, the achievable data transmission rate $r_{i,k}^{\rm M2U}$ from MU i to UAV k is described as

$$r_{i,k}^{\text{M2U}} = B_{i,k}^{\text{M2U}} \log_2(1 + \frac{h_{i,k} P_i^{\text{M2U}}}{\sigma^2}),$$
 (7)

where P_i^{M2U} denotes the transmission power of MU i, σ^2 represents the additive white Gaussian noise (AWGN). Similarly, the achievable data transmission rate $r_{i,k,j}^{\text{U2E}}$ from UAV k to EC i for the task of MU i can be written as

$$r_{i,k,j}^{\text{U2E}} = B_{i,k,j}^{\text{U2E}} \log_2(1 + \frac{h_{k,j} P_k^{\text{TX}}}{\sigma^2}),$$
 (8)

where $P_k^{\rm TX}$ denotes the transmit power of UAV k and $B_{i,k,j}^{\rm U2E}$ denotes the preset bandwidth from UAV k to EC j for MU i.

1) Communication Delay: In our system model, MUs need to offload the computation tasks to the associated UAVs for processing. The transmission delay from MU i to UAV k is expressed as

$$d_{i,k}^{\text{M2U}} = \frac{\beta_{i,k} S_i}{r_{i,k}^{\text{M2U}}}.$$
 (9)

After UAV k receives the task from MU i, it will transmit the portion $\alpha_{i,k,j}$ of the task to EC j. Therefore, the transmission delay from UAV k to EC j for the task of MU i is described as

$$d_{i,k,j}^{\text{U2E}} = \frac{\alpha_{i,k,j} S_i}{r_{i,k,j}^{\text{U2E}}}.$$
 (10)

 1 Typically, K depends on the elevation angle between the UAVs and MUs or ECs. However, for the sake of tractable analysis, this study assumes it to be constant, which has been widely adopted in UAV communication scenarios [30], [33], [34].

2) Communication Energy Consumption: For receiving the task from MU i, the communication energy consumption of UAV k can be described as

$$E_{i,k}^{\text{M2U}} = d_{i,k}^{\text{M2U}} P_k^{\text{RC}} = \frac{\beta_{i,k} S_i P_k^{\text{RC}}}{r_{i,k}^{\text{M2U}}},$$
 (11)

where $P_k^{\rm RC}$ is the receiving power of UAV k. Besides, the energy consumption of UAV k for transmitting the task of MU i to EC j can be expressed as

$$E_{i,k,j}^{\text{U2E}} = d_{i,k,j}^{\text{U2E}} P_k^{\text{TX}} = \frac{\alpha_{i,k,j} S_i P_k^{\text{TX}}}{r_{i,k,j}^{\text{U2E}}}.$$
 (12)

B. Computation Model

In this paper, we assume both UAVs and ECs adopt dynamic voltage and frequency scaling (DVFS) techniques [35], [36], which can adjust CPU-cycle frequency according to the offloaded task. After receiving the task from MU i, UAV k will assign computation resource (i.e, CPU frequency) $f_{i,k}^{\text{UAV}}$ to compute the portion $\alpha_{i,k,0}$ of the task on board. Considering the limited computation capacity of each UAV, we have

$$\sum_{i \in \mathcal{I}} f_{i,k}^{\text{UAV}} \le F_k^{\text{UAV}}, \quad \forall k, \tag{13}$$

where F_k^{UAV} is the maximum computation capacity of UAV k. Similarly, EC j will allocate computation resource $f_{i,k,j}^{\text{EC}}$ to process the portion $\alpha_{i,k,j}$ of the task from MU i via UAV k. The sum of allocated computation resources cannot exceed the total computation resources of EC j. Therefore, we have the following constraint on $f_{i,k,j}^{\text{EC}}$:

$$\sum_{k \in \mathcal{K}} \sum_{i \in \mathcal{I}} f_{i,k,j}^{\text{EC}} \le F_j^{\text{EC}}, \quad \forall j,$$
 (14)

where F_j^{EC} is the maximum computation capacity of EC j.

1) Computation Delay: The computation delay $d_{i,k}^{\mathrm{UAV}}$ for UAV k to process the task of MU i is given as

$$d_{i,k}^{\text{UAV}} = \frac{\alpha_{i,k,0} S_i C_i}{f_{i,k}^{\text{UAV}}}.$$
(15)

Likewise, the computation delay $d_{i,k,j}^{\mathrm{UAV}}$ for EC j to process the task from MU i via UAV k is written as

$$d_{i,k,j}^{\text{EC}} = \frac{\alpha_{i,k,j} S_i C_i}{f_{i,k,j}^{\text{EC}}}.$$
 (16)

2) Computation Energy Consumption: Similar to [37], the energy consumption of UAV k for processing the task of MU i is expressed as

$$E_{i,k}^{\text{UAV}} = \kappa (f_{i,k}^{\text{UAV}})^3 d_{i,k}^{\text{UAV}} = \kappa \alpha_{i,k,0} S_i C_i (f_{i,k}^{\text{UAV}})^2,$$
 (17)

where κ indicates the effective switched capacitance, which depends on the CPU architecture.

C. Problem Formulation

In this paper, we are interested in minimizing the maximal energy consumption among UAVs, while meeting the delay requirement of all tasks. To define the energy consumption of each UAV, we make the following assumptions: (i) the UAVs can execute computation and transmission in parallel; (ii) the UAVs only partition the task after receiving the entire task of associated MUs; (iii) the partition-process time is neglected in our model since it is very short compared with the entire process; (iv) UAVs and ECs only compute the task at the end of the transmission. Based on the above assumptions, the task processing delay of MU i is expressed as

$$D_{i} = \sum_{k \in \mathcal{K}} \xi_{i} \left(d_{i,k}^{\text{M2U}} + \max_{j \in \mathcal{J}} (d_{i,k}^{\text{UAV}}, d_{i,k,j}^{\text{EC}} + d_{i,k,j}^{\text{U2E}}) \right).$$
(18)

Furthermore, the total communication and computation energy consumption of UAV k to serve all MUs can be written as

$$E_k = \sum_{i \in \mathcal{I}} \xi_i (E_{i,k}^{\text{UAV}} + E_{i,k}^{\text{M2U}} + \sum_{j \in \mathcal{J}} E_{i,k,j}^{\text{U2E}}).$$
(19)

Our problem becomes jointly optimizing the M2U uplink bandwidth $B_{i,k}^{\text{M2U}}$, M2U offloading decision $\beta_{i,k}$, task partition variables $\alpha_{i,k,0}$ and $\alpha_{i,k,j}$, computation resource allocation of the UAV $f_{i,k,j}^{\text{EC}}$ and EC $f_{i,k,j}^{\text{EC}}$, and UAVs position q_k to minimize the maximal energy consumption among the UAVs, while meeting the delay requirement of all tasks. Let $\mathcal{E} = \{B_{i,k}^{\text{M2U}}, \beta_{i,k}, \alpha_{i,k,0}, \alpha_{i,k,j}, f_{i,k}^{\text{UAV}}, f_{i,k,j}^{\text{EC}}, q_k\}$. This optimization problem can be formulated as

$$\mathbf{P}_1: \quad \min_{\mathcal{E}} \quad \max_{k \in \mathcal{K}} E_k \tag{20a}$$

s.t.
$$D_i \le T$$
, $\forall i$ (20b)

$$B_{i,k}^{\text{M2U}}, f_{i,k}^{\text{UAV}} \ge 0, \quad \forall i, k$$
 (20c)

$$f_{i,k,j}^{\text{EC}} \ge 0, \quad \forall i, k, j$$
 (20d)

$$\alpha_{i,k,0}, \alpha_{i,k,j} \in [0,1], \quad \forall i,k$$
 (20e)

$$\beta_{i,k} \in \{0,1\}, \quad \forall i,k \tag{20f}$$

$$(1), (2), (3), (6), (13), (14),$$
 (20g)

where T denotes the delay requirement for tasks 2 . Constraint (20b) ensures the task is executed within the required time period. Constraints (20c) and (20d) guarantee the communication and computation resources are non-negative. Constraint (20e) states the values of partition variables are between 0 and 1. Constraint (20f) shows the offloading decisions are binary variables.

IV. SOLUTION METHODOLOGY

Problem \mathbf{P}_1 is a complicated min-max MINLP. To tackle this problem, we first utilize auxiliary variables to reformulate the original problem into a feasible one. Then, we leverage an SCA-based algorithm to solve the reformulated non-convex problem through convex approximation.

²For simplicity, we assume that the delay requirement for each task is identical. However, this assumption can be easily adapted to scenarios where the delay requirements vary for different tasks.

A. Problem Reformulation

To address the min-max problem in the objective function, we adopt the auxiliary variable $u \triangleq \max_{k \in \mathcal{K}} E_k$. Meanwhile, $v_{i,k} \triangleq \max_{j \in \mathcal{J}} (d_{i,k}^{\text{UAV}}, d_{i,k,j}^{\text{EC}} + d_{i,k,j}^{\text{U2E}})$ is defined for linearizing the task processing delay of MU i. Moreover, we relax the binary association variable $\beta_{i,k}$ into a continuous variable $\widetilde{\beta}_{i,k} \in [0,1]$. Finally, the problem \mathbf{P}_1 can be reformulated as

$$\mathbf{P}_2: \quad \min_{\{\mathcal{E}, u, v_{i,k}\}} \quad u \tag{21a}$$

s.t.
$$u \ge E_k$$
, $\forall k$ (21b)

$$v_{i,k} \ge d_{i,k}^{\text{UAV}}, \quad \forall i, k$$
 (21c)

$$v_{i,k} \geq d_{i,k,j}^{\text{EC}} + d_{i,k,j}^{\text{U2E}}, \quad \forall i,k,j \tag{21d} \label{eq:21d}$$

$$T_i \ge \sum_{k \in \mathcal{K}} \xi_i (d_{i,k}^{\text{M2U}} + v_{i,k}), \quad \forall i, k$$
 (21e)

$$\sum_{k \in \mathcal{K}} \widetilde{\beta}_{i,k} = 1, \quad \forall i$$
 (21f)

$$0 \le \widetilde{\beta}_{i,k} \le 1, \quad \forall i, k \tag{21g}$$

$$\alpha_{i,k,0} + \sum_{j \in \mathcal{J}} \alpha_{i,k,j} = \widetilde{\beta}_{i,k}, \quad \forall k, i$$
 (21h)

$$(3), (6), (13), (14), (20c), (20d), (20e).$$
 (21i)

However, P_2 is still hard to solve due to the non-convex constraints (21b), (21c), (21d) and (21e).

B. Successive Convex Approximation

Instead of expensive searching for the globally optimized solution, we develop an SCA-based algorithm to address the non-convex problem. To generate proper convex approximations, we utilize the following lemmas:

Lemma 1 (Example 3 in [38]): Consider a non-convex constraint $g(x) \leq 0$ which satisfies the SCA condition [38, Assumption 3] and can be written as $g(x) = h_1(x) - h_2(x)$ with continuously differentiable convex h_1 and h_2 . For any y in the domain of g(x), we can linearize the concave part $-h_2(x)$ and write the convex upper approximation of g(x) as

$$g(\boldsymbol{x}) \leq \widetilde{g}(\boldsymbol{x}; \boldsymbol{y}) \triangleq h_1(\boldsymbol{x}) - h_2(\boldsymbol{y}) - \nabla_{\boldsymbol{x}} h_2(\boldsymbol{y})^{\top} (\boldsymbol{x} - \boldsymbol{y}).$$
 (22)

Lemma 2 (Example 4 in [38]): Consider a non-convex constrain $g(x) \leq 0$ which satisfies the SCA condition [38, Assumption 3] and can be written as $g(x) = f_1(x)f_2(x)$ with differentiable convex non-negative f_1 and f_2 . For any y in the domain of g(x), the convex upper approximation of g(x) is given as

$$g(x) \leq \widetilde{g}(x; y) \triangleq \frac{1}{2} (f_1(x) + f_2(x))^2 - \frac{1}{2} (f_1^2(y) + f_2^2(y)) - f_1(y) f_1'(y) (x - y) - f_2(y) f_2'(y) (x - y)$$
(23)

Based on the above lemmas, the non-convex terms $d_{i,k}^{\mathrm{UAV}}$ in constraint (21c) can be written as

$$d_{i,k}^{\text{UAV}} = S_i C_i f_1(\alpha_{i,k,0}) f_2(f_{i,k}^{\text{UAV}}), \tag{24}$$

where $f_1(\alpha_{i,k,0}) = \alpha_{i,k,0}$ and $f_2(f_{i,k}^{\text{UAV}}) = 1/f_{i,k}^{\text{UAV}}$. Given the feasible solutions $\alpha_{i,k,0}(n)$ and $f_{i,k}^{\text{UAV}}(n)$ for the n-th

iteration of SCA-based algorithm, we can derive a convex upper approximation of $d_{i,k}^{\text{UAV}}$ by utilizing Lemmas 2 as

$$\begin{aligned} d_{i,k}^{\text{UAV}} &\leq \widetilde{d}_{i,k}^{\text{UAV}} \left(\alpha_{i,k,0}, f_{i,k}^{\text{UAV}}; \alpha_{i,k,0}(n), f_{i,k}^{\text{UAV}}(n)\right) \triangleq S_i C_i \\ \frac{1}{2} \left(\left(\alpha_{i,k,0} + \frac{1}{f_{i,k}^{\text{UAV}}}\right)^2 - \left(\alpha_{i,k,0}(n)\right)^2 - \left(\frac{1}{f_{i,k}^{\text{UAV}}(n)}\right)^2 \right) - \\ \alpha_{i,k,0}(n) \left(\alpha_{i,k,0} - \alpha_{i,k,0}(n)\right) + \left(\frac{1}{f_{i,k}^{\text{UAV}}(n)}\right)^3 \left(f_{i,k}^{\text{UAV}} - f_{i,k}^{\text{UAV}}(n)\right) \\ + \left(f_{i,k}^{\text{UAV}}(n)\right) \right]. \end{aligned} \tag{25}$$

In the non-convex constraint (21d), $d_{i,k,j}^{\text{U2E}}$ can be written as a product of S_i , $\alpha_{i,k,j}$ and $1/r_{i,k,j}^{\text{U2E}}$. We cannot directly apply Lemma 2 since $1/r_{i,k,j}^{\text{U2E}}$ is non-convex. To address this non-convexity, we define non-negative auxiliary variables $\phi_{i,k,j}$ to replace $r_{i,k,j}^{\text{U2E}}$ and obtain the following:

$$d_{i,k,j}^{U2E} = S_i f_1(\alpha_{i,k,j}) f_2(\phi_{i,k,j}), \tag{26}$$

where $f_1(\alpha_{i,k,j}) = \alpha_{i,k,j}$ and $f_2(\phi_{i,k,j}) = 1/\phi_{i,k,j}$. Then, we can leverage Lemmas 2 and the feasible solutions $\alpha_{i,k,j}(n)$, $\phi_{i,k,j}(n)$ of problem \mathbf{P}_2 to derive a convex upper approximation of $d_{i,k,j}^{\mathrm{U2E}}$ for the n-th iteration of SCA-based algorithm:

$$d_{i,k,j}^{U2E} \leq \widetilde{d}_{i,k,j}^{U2E} \left(\alpha_{i,k,j}, \phi_{i,k,j}; \alpha_{i,k,j}(n), \phi_{i,k,j}(n)\right) \triangleq S_{i} \begin{bmatrix} \frac{1}{2} \left(\left(\alpha_{i,k,j} + \frac{1}{\phi_{i,k,j}}\right)^{2} - \left(\alpha_{i,k,j}(n)\right)^{2} - \left(\frac{1}{\phi_{i,k,j}(n)}\right)^{2}\right) - \alpha_{i,k,j}(n) \left(\alpha_{i,k,j} - \alpha_{i,k,j}(n)\right) + \left(\frac{1}{\phi_{i,k,j}(n)}\right)^{3} \left(\phi_{i,k,j} - \phi_{i,k,j}(n)\right) \end{bmatrix}.$$

$$(27)$$

Similarly, we rewrite the non-convex term $d_{i,k,j}^{\mathrm{EC}}$ in constraint (21d) as

$$d_{i,k,j}^{EC} = S_i C_i f_1(\alpha_{i,k,j}) f_2(f_{i,k,j}^{EC}), \tag{28}$$

where $f_1(\alpha_{i,k,j}) = \alpha_{i,k,j}$ and $f_2(f_{i,k,j}^{\rm EC}) = 1/f_{i,k,j}^{\rm EC}$. By applying Lemma 2 and utilizing the feasible solutions $\alpha_{i,k,j}(n)$, $f_{i,k,j}^{\rm UAV}(n)$ of problem \mathbf{P}_2 , we can derive a convex upper approximation of $d_{i,k,j}^{\rm EC}$ for the n-th iteration of SCA-based algorithm:

$$d_{i,k,j}^{\text{EC}} \leq \widetilde{d}_{i,k,j}^{\text{EC}} \left(\alpha_{i,k,j}, f_{i,k}^{\text{UAV}}; \alpha_{i,k,j}(n), f_{i,k,j}^{\text{UAV}}(n)\right) \triangleq S_i C_i \left[\frac{1}{2} \left(\left(\alpha_{i,k,j} + \frac{1}{f_{i,k,j}^{\text{EC}}}\right)^2 - \left(\alpha_{i,k,j}(n)\right)^2 - \left(\frac{1}{f_{i,k,j}^{\text{EC}}(n)}\right)^2\right) - \alpha_{i,k,j}(n) \left(\alpha_{i,k,j} - \alpha_{i,k,j}(n)\right) + \left(\frac{1}{f_{i,k,j}^{\text{EC}}(n)}\right)^3 \left(f_{i,k,j}^{\text{EC}} - f_{i,k,j}^{\text{EC}}(n)\right)\right].$$

$$(29)$$

To process the non-convex term $d_{i,k}^{M2U}$ in constraint (21e), we define $\bar{r}_{i,k}^{M2U} \triangleq \log_2(1 + \frac{h_{i,k}P_i^{MU}}{\sigma^2})$ and substitute it with a non-negative auxiliary variable $\mu_{i,k}$, then rewrite the nonconvex term $d_{i,k}^{M2U}$ as

$$d_{i,k}^{\text{M2U}} = \frac{1}{2} S_i \bigg[\underbrace{(\frac{1}{B_{i,k}^{\text{M2U}} \mu_{i,k}} + \beta_{i,k})^2}_{h_1} \underbrace{-(\frac{1}{B_{i,k}^{\text{M2U}} \mu_{i,k}})^2 - (\beta_{i,k})^2}_{h_2} \bigg].$$

(30)

Note that h_1 is convex and h_2 is concave in (30), which satisfies the requirement of Lemma 1. Given the feasible solutions $B_{i,k}^{\text{M2U}}(n)$, $\mu_{i,k}(n)$, and $\beta_{i,k}(n)$ of problem \mathbf{P}_2 , we can derive a convex upper approximation of $d_{i,k}^{M2U}$ for the n-th iteration of SCA-based algorithm as

$$\begin{split} & d_{i,k}^{\text{M2U}} \leq \widetilde{d}_{i,k}^{\text{M2U}} \left(B_{i,k}^{\text{M2U}}, \mu_{i,k}, \beta_{i,k}; B_{i,k}^{\text{M2U}}(n), \mu_{i,k}(n), \beta_{i,k}(n) \right) \triangleq \\ & S_{i} \left[\frac{1}{2} \left(\left(\frac{1}{B_{i,k}^{\text{M2U}} \mu_{i,k}} + \beta_{i,k} \right)^{2} - \left(\frac{1}{B_{i,k}^{\text{M2U}}(n) \mu_{i,k}(n)} \right)^{2} - \left(\beta_{i,k}(n) \right)^{2} \right) - \left(\beta_{i,k}(n) \right) \left(\beta_{i,k} - \beta_{i,k}(n) \right) + \\ & \frac{\left(B_{i,k}^{\text{M2U}} - B_{i,k}^{\text{M2U}}(n) \right)}{\left(B_{i,k}^{\text{M2U}}(n) \right)^{3} \left(\mu_{i,k}(n) \right)^{2}} + \frac{\left(\mu_{i,k} - \mu_{i,k}(n) \right)}{\left(\mu_{i,k}(n) \right)^{3} \left(B_{i,k}^{\text{M2U}}(n) \right)^{2}} \right]. \end{split}$$
(31)

Moreover, we can rewrite the non-convex term $E_{i.k}^{\mathrm{UAV}}$ in constraint (21b) as

$$E_{ik}^{\text{UAV}} = \kappa S_i C_i f_1(\alpha_{i,k,0}) f_3(f_{ik}^{\text{UAV}}),$$
 (32)

where $f_1(\alpha_{i,k,0})=\alpha_{i,k,0}$ and $f_3(f_{i,k}^{\text{UAV}})=(f_{i,k}^{\text{UAV}})^2$. Using Lemma 2 and the feasible solutions $\alpha_{i,k,0}(n)$ and $f_{i,k}^{\text{UAV}}(n)$ of problem P_2 , we can derive a convex upper approximation of $E_{i,k}^{\text{UAV}}$ for the *n*-th iteration of SCA-based algorithm as

$$\begin{split} E_{i,k}^{\text{UAV}} &\leq \widetilde{E}_{i,k}^{\text{UAV}} \Big(\alpha_{i,k,0}, f_{i,k}^{\text{UAV}}; \alpha_{i,k,0}(n), f_{i,k}^{\text{UAV}}(n)\Big) \triangleq \kappa S_i C_i \Bigg[\\ \frac{1}{2} \Bigg(\Big(\alpha_{i,k,0} + (f_{i,k}^{\text{UAV}})^2\Big)^2 - \Big(\alpha_{i,k,0}(n)\Big)^2 - \Big(f_{i,k}^{\text{UAV}}(n)\Big)^4 \Bigg) - \\ \alpha_{i,k,0}(n) \Big(\alpha_{i,k,0} - \alpha_{i,k,0}(n)\Big) - 2 \Big(f_{i,k}^{\text{UAV}}(n)\Big)^3 \Big(f_{i,k}^{\text{UAV}} - f_{i,k}^{\text{UAV}}(n)\Big) \Bigg]. \end{split}$$

$$(33)$$

Additionally, we represent the convex upper approximation of non-convex terms $E_{i,k}^{\text{M2U}}$ and $E_{i,k,j}^{\text{U2E}}$ using the derived $\widetilde{d}_{i,k}^{\text{M2U}}$ and $\widetilde{d}_{i,k,j}^{\text{U2E}}$:

$$E_{i,k}^{\text{M2U}} \leq \widetilde{E}_{i,k}^{\text{M2U}} \triangleq \widetilde{d}_{i,k}^{\text{M2U}} P_k^{\text{RC}}, \tag{34}$$
$$E_{i,k,j}^{\text{U2E}} \leq \widetilde{E}_{i,k,j}^{\text{U2E}} \triangleq \widetilde{d}_{i,k,j}^{\text{U2E}} P_k^{\text{TX}}. \tag{35}$$

$$E_{i,k,j}^{\text{U2E}} \le \widetilde{E}_{i,k,j}^{\text{U2E}} \triangleq \widetilde{d}_{i,k,j}^{\text{U2E}} P_k^{\text{TX}}.$$
 (35)

Then, we obtain the convex approximation of the UAV energy consumption E_k as

$$\widetilde{E}_{k} \triangleq \sum_{i \in \mathcal{I}} \xi_{i} (\widetilde{E}_{i,k}^{\text{UAV}} + \widetilde{E}_{i,k}^{\text{M2U}} + \sum_{j \in \mathcal{J}} \widetilde{E}_{i,k,j}^{\text{U2E}}).$$
(36)

Recall that we utilize auxiliary variables $\mu_{i,k}=\bar{r}_{i,k}^{\text{M2U}}$ and $\phi_{i,k,j}=r_{i,k,j}^{\text{U2E}}$. In order to further tackle this non-convex problem, we relax the auxiliary variables as

$$0 \le \mu_{i,k} \le \bar{r}_{i,k}^{\text{M2U}},\tag{37}$$

$$0 \le \mu_{i,k} \le \bar{r}_{i,k}^{M2U}, \tag{37}$$

$$0 \le \phi_{i,k,j} \le r_{i,k,j}^{U2E}. \tag{38}$$

Note that $\bar{r}_{i,k}^{\text{M2U}}$ and $r_{i,k,j}^{\text{U2E}}$ are non-negative convex functions with respect to $\left\| \boldsymbol{Q}_i - \boldsymbol{q}_k \right\|^2$ and $\left\| \boldsymbol{Q}_j - \boldsymbol{q}_k \right\|^2$. Given the feasible solutions $q_k(n)$ of problem P_2 , we can leverage the first-order Taylor expansions of $\bar{r}_{i,k}^{\text{M2U}}$ and $r_{i,k,j}^{\text{U2E}}$ as their lower bounds for the n-th iteration of SCA-based algorithm [39]:

$$\bar{r}_{i,k}^{\text{M2U}} \geq \bar{r}_{i,k,\text{LB}}^{\text{M2U}} \left(\boldsymbol{q}_{k}; \boldsymbol{q}_{k}(n) \right) \triangleq \bar{r}_{i,k}^{\text{M2U}} \left(\boldsymbol{q}_{k}(n) \right)$$

$$- \frac{\zeta_{i,k} \left(\left\| \boldsymbol{Q}_{i} - \boldsymbol{q}_{k} \right\|^{2} - \left\| \boldsymbol{Q}_{i} - \boldsymbol{q}_{k}(n) \right\|^{2} \right)}{\ln 2 \left(\left\| \boldsymbol{Q}_{i} - \boldsymbol{q}_{k}(n) \right\|^{2} \right) \left(\zeta_{i,k} + \left\| \boldsymbol{Q}_{i} - \boldsymbol{q}_{k}(n) \right\|^{2} \right)}, \quad (39)$$

where
$$\zeta_{i,k} \triangleq h_0 P_i^{\text{M2U}} \left(\sqrt{\frac{K}{K+1}} + \sqrt{\frac{1}{K+1}} g_{k,j} \right)^2 / \sigma^2$$
 and

$$r_{i,k,j}^{\text{U2E}} \geq r_{i,k,j,\text{LB}}^{\text{U2E}} \left(\boldsymbol{q}_{k}; \boldsymbol{q}_{k}(n) \right) \triangleq \bar{r}_{i,k,j}^{\text{U2E}} \left(\boldsymbol{q}_{k}(n) \right)$$

$$- \frac{B_{i,k,j}^{\text{U2E}} \eta_{k} \left(\left\| \boldsymbol{Q}_{j} - \boldsymbol{q}_{k} \right\|^{2} - \left\| \boldsymbol{Q}_{j} - \boldsymbol{q}_{k}(n) \right\|^{2} \right)}{\ln 2 \left(\left\| \boldsymbol{Q}_{j} - \boldsymbol{q}_{k}(n) \right\|^{2} \right) \left(\eta_{k,j} + \left\| \boldsymbol{Q}_{j} - \boldsymbol{q}_{k}(n) \right\|^{2} \right)}, \quad (40)$$

where $\eta_{k,j} \triangleq h_0 P_k^{\text{TX}} \left(\sqrt{\frac{K}{K+1}} + \sqrt{\frac{1}{K+1}} g_{k,j} \right)^2 / \sigma^2$. Then we can obtain the approximated convex constraints by replace $\bar{r}_{i,k}^{\text{M2U}}$ and $r_{i,k,j}^{\text{U2E}}$ with their lower bounds in (37) and (38):

$$0 \le \mu_{i,k} \le \bar{r}_{i,k,LB}^{M2U} (\boldsymbol{q}_k; \boldsymbol{q}_k(n)), \tag{41}$$

$$0 \le \phi_{i,k,j} \le r_{i,k,j,\text{LB}}^{\text{U2E}} \left(\boldsymbol{q}_k; \boldsymbol{q}_k(n) \right). \tag{42}$$

Note that $\|\mathbf{q}_{k'} - \mathbf{q}_k\|^2$ are convex with respect to $(\mathbf{q}_{k'} - \mathbf{q}_k)$. Similarly, given two feasible UAV positions $q_{k'}(n)$ and $q_k(n)$, we apply the first-order Taylor expansion to $\|oldsymbol{q}_{k'} - oldsymbol{q}_k\|^2$ and obtain its lower bound for the n-th iteration of SCA-based algorithm [39]:

$$\|\boldsymbol{q}_{k'} - \boldsymbol{q}_{k}\|^{2} \ge L_{k',k,LB} \left(\boldsymbol{q}_{k'}, \boldsymbol{q}_{k}; \boldsymbol{q}_{k'}(n), \boldsymbol{q}_{k}(n)\right) \triangleq -\|\boldsymbol{q}_{k'}(n) - \boldsymbol{q}_{k}(n)\|^{2} + 2\left(\boldsymbol{q}_{k'}(n) - \boldsymbol{q}_{k}(n)\right)^{\top} \left(\boldsymbol{q}_{k'} - \boldsymbol{q}_{k}\right). \tag{43}$$

Finally, we define the set of decision variables as $\psi =$ $(B^{\text{M2U}}_{i,k}, \overset{\sim}{\beta_{i,k}}, \alpha_{i,k,0}, \alpha_{i,k,j}, f^{\text{UAV}}_{i,k}, f^{\text{EC}}_{i,k,j}, \boldsymbol{q}_k, \mu_{i,k}, \phi_{i,k,j}, u, v_{i,k}).$ Given a feasible solution $\psi(n)$ of problem \mathbf{P}_2 for the n-th

Algorithm 1 SCA-based algorithm

Input: Initialize $\psi(0)$. Set $n=0, \gamma=0.5, \theta(n)\in(0,1]$, and a threshold δ .

1: repeat

2: Compute $\hat{\psi}(\psi(n))$, the solution of problem \mathbf{P}_3 ;

3: Set $\psi(n+1) = \psi(n) + \theta(n)(\hat{\psi}(\psi(n)) - \psi(n))$, with $\theta(n) = \theta(n-1)(1-\gamma\theta(n))$;

4: Set $n \leftarrow n + 1$.

5: **until** $\|\psi(n+1) - \psi(n)\| \le \delta$

Output: ψ^* .

iteration of the SCA-based algorithm, we reformulated problem \mathbf{P}_2 as

$$\begin{aligned} \mathbf{P}_{3} : & \min_{\psi} \quad u & \text{(44a)} \\ \text{s.t.} \quad u & \geq \sum_{i \in \mathcal{I}} \xi_{i} \bigg(\widetilde{E}_{i,k}^{\text{UAV}} \Big(\psi; \psi(n) \Big) + \widetilde{E}_{i,k}^{\text{M2U}} \Big(\psi; \psi(n) \Big) \\ & + \sum_{j \in \mathcal{J}} \widetilde{E}_{i,k,j}^{\text{U2E}} \Big(\psi; \psi(n) \Big) \bigg), \quad \forall k & \text{(44b)} \\ & v_{i,k} & \geq \widetilde{d}_{i,k}^{\text{UAV}} \Big(\psi; \psi(n) \Big), \quad \forall i, k & \text{(44c)} \\ & v_{i,k} & \geq \widetilde{d}_{i,k,j}^{\text{EC}} \Big(\psi; \psi(n) \Big) + \widetilde{d}_{i,k,j}^{\text{U2E}} \Big(\psi; \psi(n) \Big), \end{aligned}$$

$$\forall i, k, j \tag{44d}$$

$$T > \sum_{i} \int_{\mathbb{R}^{2}} \widetilde{\mathcal{A}}^{M2U}(s_{i}, s_{i}, s_{i}) + s_{i} \qquad \forall i, k$$

$$T_{i} \ge \sum_{k \in \mathcal{K}} \xi_{i} \left(\widetilde{d}_{i,k}^{\text{M2U}} \left(\psi; \psi(n) \right) + v_{i,k} \right), \quad \forall i, k$$
(44e)

$$L_{k',k,\mathrm{LB}}(\psi;\psi(n)) \ge L^{\min}, \quad \forall k' \ne k$$
 (44f)

$$0 \le \mu_{i,k}^{M2U} \le \overline{r}_{i,k,\text{LB}}^{M2U} \Big(\psi; \psi(n) \Big), \quad \forall i, k$$
 (44g)

$$0 \le \phi_{i,k,j}^{U2E} \le r_{i,k,j,\text{LB}}^{\text{U2E}} \Big(\psi; \psi(n) \Big), \quad \forall i, k, j \quad \text{(44h)}$$

$$(6), (13), (14), (20c) - (20e), (21f) - (21h).$$
 (44i)

The problem P_3 is a convex problem that can be easily solved by the interior point method (IPM) [39]. We denote the solution of this problem as $\psi(\psi(n))$ and summarize the SCAbased algorithm in Algorithm 1. The proof for the convergence of SCA can be found in [40], and the algorithm will terminate after a finite number of iterations if a suboptimal solution exists. If the association variable $\beta_{i,k}$ in the solution of problem P_3 is integer, this means that the solution of problem P_1 has also been found. However, if the association variable $\beta_{i,k}$ in the solution of problem P_3 is fractional, we cannot simply round it off, as such solutions are not desirable and may even be infeasible. Therefore, we develop a binary variables recovery algorithm to obtain the approximated integer solution for problem P_1 . In each iteration of the algorithm, we round off the largest $\beta_{i,k}$ to 1, because such an association is more likely to be the optimal one. The details of the binary variables recovery algorithm are shown in Algorithm 2.

V. NUMERICAL EXPERIMENTS

In this section, we conduct extensive numerical experiments to evaluate the performance of our proposed SCA-based algo**Algorithm 2** Binary variables recovery algorithm for problem **P**₁

Input: Set $\mathcal{M} = \emptyset$, j = 0.

- 1: while $j \leq I$ do
- 2: Solve the problem \mathbf{P}_3 using Algorithm 1 with fixed $\{\widetilde{\beta}_{i,k} = 1 | i \in \mathcal{M}, k \in \mathcal{K}\}$ and obtain $\psi(j)$.
- 3: Find the maximum decision value $\{\widetilde{\beta}_{\tilde{i},k}|\tilde{i}\in\mathcal{I}\setminus\mathcal{M},k\in\mathcal{K}\}$.
- 4: Set $\mathcal{M} = \mathcal{M} \cup \tilde{i}$.
- 5: Set j = j + 1;
- 6: end while

Output: $\psi *$ with the recovered binary variables $\{\beta_{i,k} = 1 | i \in \mathcal{M}, k \in \mathcal{K}\}$ and $\{\beta_{i,k} = 0 | i \in \mathcal{I} \setminus \mathcal{M}, k \in \mathcal{K}\}$

rithm. All simulations are implemented in MATLAB R2020a running on a desktop computer with a 3.2 GHz Intel^R CoreTM i7-8700 CPU and 16 GB of RAM with CVX [43].

A. Simulation Setup

In our simulation, a $1 \times 1 \text{ km}^2$ square area is considered, where 30 MUs are uniformly distributed, and 4 ECs are located at each vertex. In order to guarantee the MUs complete their tasks within the time period T=2.5 s, 3 UAVs hover at the fixed altitude H=100 m to provide relaying and computation services. Unless otherwise specified, the rest of our simulation parameters are given in Table I.

As stated in Section I, our system setting, which comprises multiple UAVs, ground MUs, and ECs, is different from prior works. Moreover, our objective is also unique. Their proposed approaches can not be directly applied to our scenario. Therefore, we set four special cases as baselines: 1) Random UAV position scheme (RUP): The UAVs are randomly deployed without optimization; 2) Fixed computation resource allocation scheme (FCP): The computation resources of each UAV are equally allocated to each task; 3) Fixed communication resource allocation scheme (FCM): The communication resources of each UAV are equally allocated to MUs; 4) Fixed task splitting decisions scheme (FTS): The portions of tasks that are processed at UAVs and ECs are equal. Note that the baseline schemes also leverage the proposed algorithm to optimize other variables.

B. Experimental Results

In this section, we first demonstrate the performance of the proposed multi-UAV-enabled MEC system. Then, we analyze

TABLE I: simulation parameters

| Parameters | Values | Parameters | Values |
|----------------------|-------------------------|--------------------------|--------------|
| P_k^{RC} | 0.1 W | P_k^{TX} | 1 W |
| $\widetilde{\delta}$ | 10^{-3} | \tilde{T} | 2.5 s |
| κ | 10^{-28} [41], [42] | S_i | [1,10] Mbits |
| C_i | [50,200] CPU cycles/bit | $\frac{\xi_i}{\sigma^2}$ | 30 tasks/min |
| h_0 | -50 dB | | -100 dBm |
| F_k^{UAV} | 3 GHz | F_i^{EC} | [15,30] GHz |
| $B_k^{	ext{M2U}}$ | 10 MHz | $B_{i,k,j}^{ m U2E}$ | 1 MHz |
| L^{\min} | 10 m | | |

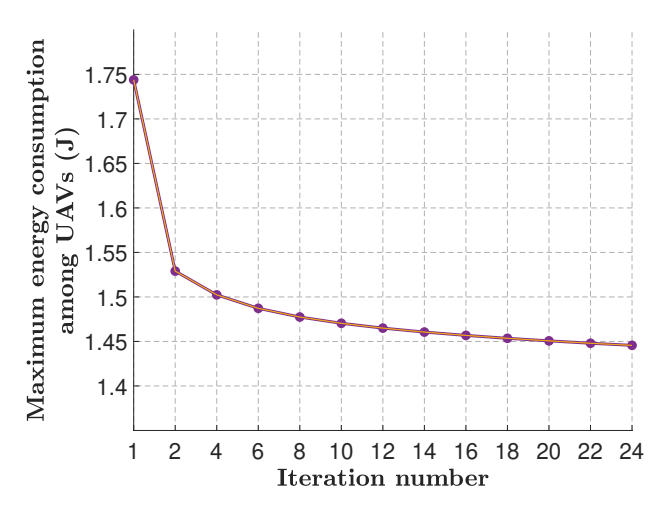


Fig. 2: Convergence of algorithm 1.

the impacts of various parameters on the system performance. Finally, we compare our proposed multi-UAV-enabled MEC system with the four baselines.

1) Performance of the multi-UAV-enabled MEC system: Fig. 2 depicts the convergence of algorithm 1. As the tendency shows, we keep optimizing the maximum energy consumption among UAVs until reaching the stationary status. Fig. 3 demonstrates the optimal position of UAVs in the proposed system, where various colors represent the different associations between UAVs and MUs. Particularly, we can obtain the optimal position of UAVs with corresponding UAV coordinates: (334, 490, 100), (619, 652, 100), and (564, 302, 100). Furthermore, Figure 4 illustrates the optimal ratios for executing tasks in UAVs and ECs. As shown, the UAVs can independently process small tasks (e.g., 1 Mbits from MU 15). However, for large tasks (e.g., 10 Mbits from MU 2), a collaboration between the UAVs and ECs is necessary to ensure the tasks are completed in time.

2) Impact of the delay requirement: In this part, we investigate how the delay requirement of tasks affects the

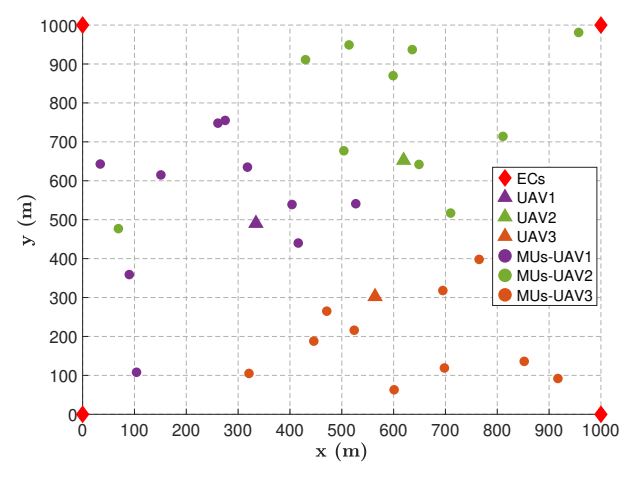


Fig. 3: Simulation result of the proposed multi-UAV-enabled MEC system (I=30,K=3,J=4).

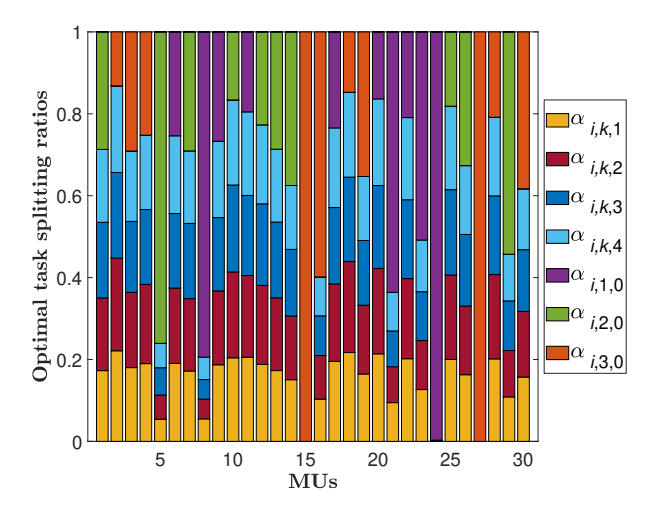


Fig. 4: Optimal task splitting ratios of the UAVs $\alpha_{i,k,0}$ and ECs $\alpha_{i,k,j}$ (k=1,2,3,j=1,2,3,4) for MUs i $(i=1,2,\ldots,30)$.

system performance in terms of the total energy consumption, communication, and computation energy consumption for each UAV. From Fig. 5(a), we can observe the total energy consumption of each UAV remains at the same level across various delay requirements. This result verifies that our proposed algorithm can achieve min-max fairness of energy consumption among UAVs under different delay requirements. Meanwhile, Fig. 5(a) also indicates the total energy consumption of each UAV decreases as the delay requirement increases. As mentioned in Section III, the total energy consumption comprises the communication and computation energy consumption. Fig. 5(b) and Fig. 5(c) further demonstrate the details of this. These two figures show that the computation energy consumption increases, while the communication energy consumption decreases as the delay requirement increases. The reason is that the total tasks cannot be processed on the UAVs when the value of the delay requirement is small. The UAVs have to further offload a large portion of tasks that exceed their computing capacity to the ECs. When the delay requirement increases, the UAVs have more time to process tasks onboard, which enables them to offload fewer tasks to the ECs. Moreover, these two figures also depict that the communication and computation energy consumption experience a slight fluctuation. The main reason is that our objective is to minimize the maximal total energy consumption among UAVs. Even though the value of objective function monotonously decreases, the components (i.e., computation and communication energy consumption) may fluctuate.

3) Impact of single UAV transmission power: In this part, we study the impact of a single UAV transmission power on the system performance in terms of total energy consumption, communication, and computation energy consumption. To that end, we increase the transmission power of UAV 3 from 1 to 5 W, while keeping the transmission powers of the other two UAVs unchanged. As demonstrated in Fig. 6(a), the total energy consumption of each UAV increases as the transmission power of UAV 3 increases. This is due to the fact that U2E energy consumption is an increasing function

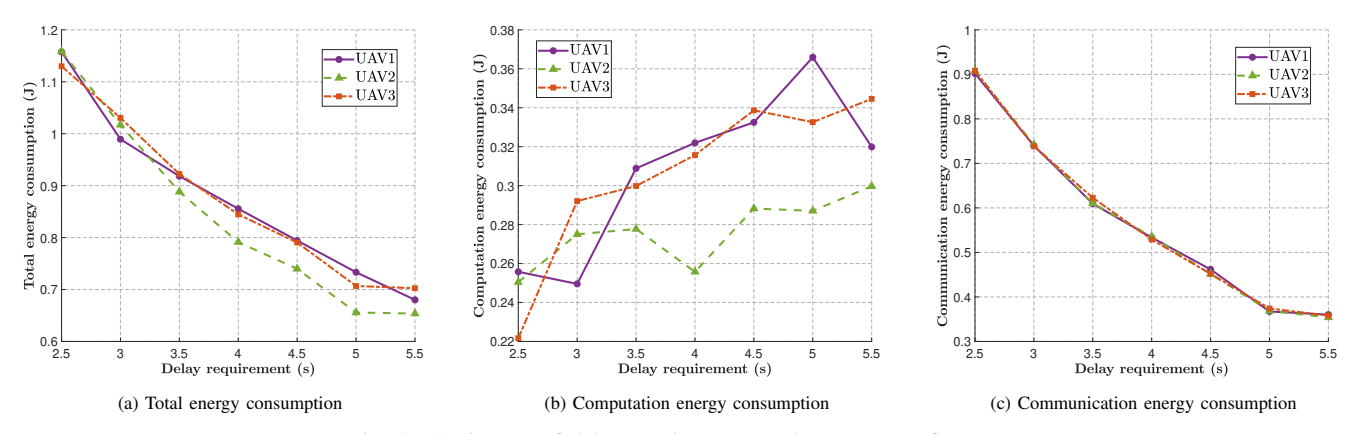


Fig. 5: The impact of delay requirement on the system performance.

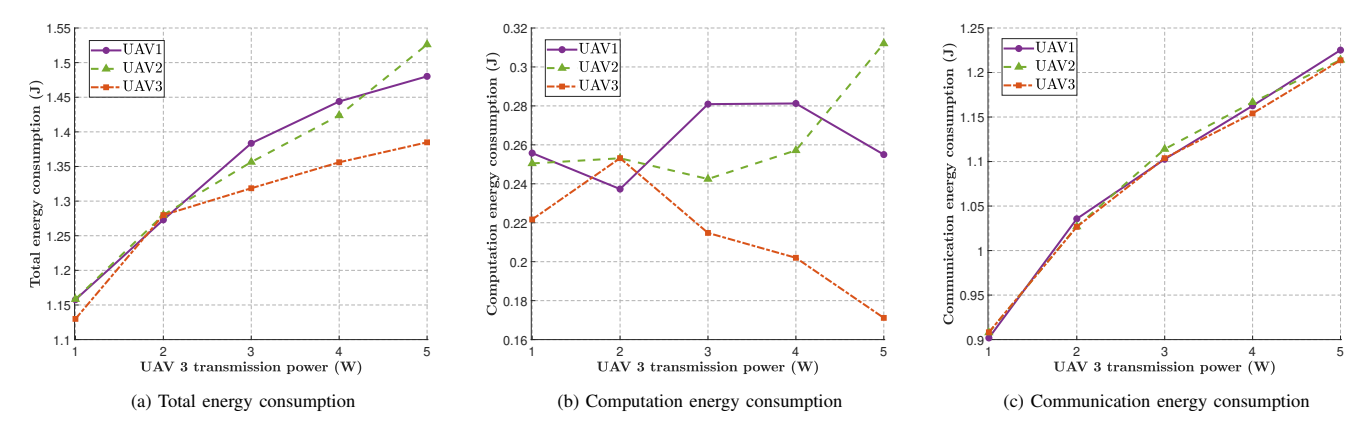


Fig. 6: The impact of UAV 3 transmission power on the system performance.

of the UAV's transmission power. As the transmission power of UAV 3 increases, it consumes more energy to offload the same task to the ECs. To mitigate this energy cost, more tasks are offloaded to the other two UAVs, and fewer tasks are offloaded to UAV 3. Specifically, as shown in Fig. 6(b), we can observe that the computation energy consumption of UAV 3 reduces, while such energy consumption of the other two UAVs slightly increases as the transmission power of UAV 3 increases. Moreover, unlike the significant fluctuation in computation energy consumption shown in Fig. 6(b), Fig. 6(c) indicates that the communication energy consumption of each UAV monotonously increases as the transmission power of UAV 3 increases. The reason is that the communication energy consumption of each UAV dominates its overall energy consumption.

4) Benefits of the multi-UAV-enabled MEC system: In this part, we compare the system performance of the proposed scheme with different baselines in terms of reducing the maximum energy consumption among UAVs. Specifically, we investigate how maximum energy consumption among UAVs behaves as the delay requirement and a single UAV transmission power change, respectively. As depicted in Fig. 7, our proposed multi-UAV-enabled MEC scheme has the lowest maximum energy consumption among all schemes under

various delay requirements. Particularly, the proposed scheme can save up to 4.2%, 4.4%, 27.1%, and 59.0%, compared with RUP, FCP, FCM, and FTS on maximum energy consumption among UAVs, respectively. Furthermore, we observe that the maximum energy consumption among UAVs of all schemes decreases as the delay requirement increases, except for FTS, which remains unchanged. The reason for this observation is that the computation capacity of ECs is not fully utilized when the task-splitting ratio is fixed. It also indicates that optimizing the collaboration between UAVs and ECs brings crucial performance gains. Moreover, we can see that RUP and FCP perform better than the FCM. The reason is that communication energy consumption dominates the overall energy consumption and significantly affects the system performance. Next, we explore how the system performance changes as the transmission power of UAV 3 increases from 1 to 5 W. Fig. 8 shows that the proposed scheme performs best among all schemes in the various UAV 3 transmission power settings. Specifically, the proposed scheme can save up to 9.8%, 5.1%, 25.2%, and 37.4%, compared with RUP, FCP, FCM, and FTS on maximum energy consumption among UAVs, respectively. Additionally, we can observe that the maximum energy consumption among UAVs increases as the transmission power of UAV 3 increases. From the above two

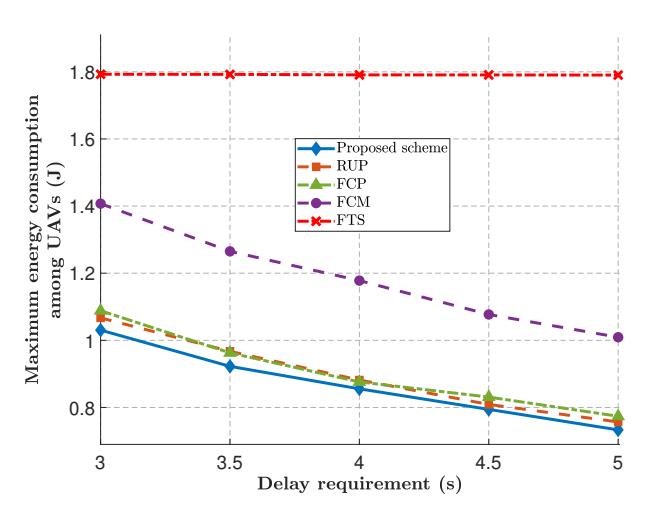


Fig. 7: Maximum energy consumption among UAVs as a function of delay requirement assigned to tasks

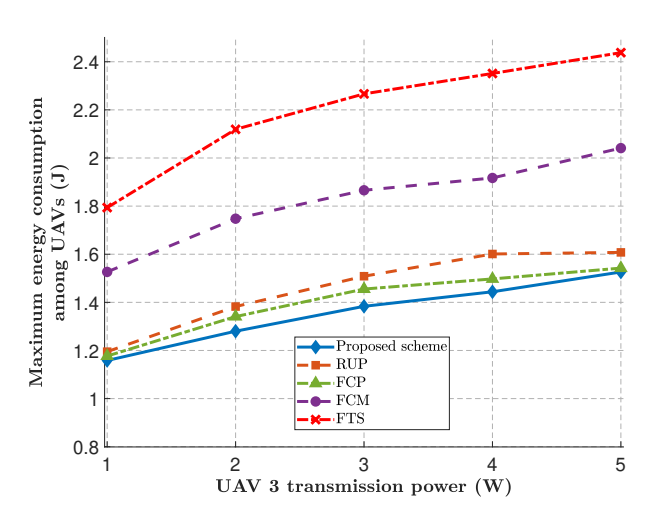


Fig. 8: Maximum energy consumption among UAVs as a function of UAV 3 transmission power $P_{i,3,j}^{\mathrm{TX}}$ $(j=1,\ldots,4$ and $i=1,2,\ldots,30)$ while fixing the others at 1 W.

simulation results, it can be seen that our proposed scheme significantly outperforms others in reducing the maximum energy consumption among UAVs, which verifies the benefits of the proposed scheme in processing computation-intensive and latency-critical tasks.

VI. CONCLUSION

In this paper, we have proposed a multi-UAV-enabled MEC architecture where multiple UAVs are deployed to facilitate the communication and computation of ground IoT devices in signal-blocked and shadowed environments. In order to achieve the min-max fairness of energy consumption among UAVs and prolong the service cycle for the multi-UAV-enabled MEC system, we have formulated an optimization problem to minimize the maximal energy consumption among UAVs by jointly optimizing computation offloading decisions, communication and computation resource allocation, UAV positions, and task splitting decisions while meeting the delay

requirement of all tasks. The resulting optimization problem is MINLP, which is hard to solve. To tackle this problem, we have designed an efficient SCA-based algorithm to obtain a suboptimal solution. Numerical results show that our proposed multi-UAV-enabled MEC scheme outperforms various baseline schemes in processing computation-intensive and latency-critical tasks. The proposed scheme can provide valuable insights into the cooperation between UAVs and ground ECs in the next-generation wireless networks. In the future, we will extend our work to the energy-efficient multi-UAV-enabled MEC design considering UAV trajectory.

VII. ACKNOWLEDGEMENTS

The work of Y. Zhang, Y. Guo, and Y. Gong was partially supported by NSF under grants CNS-2047761, CNS-2106761, and CNS-2318663.

REFERENCES

- "Connected devices will generate 79 zettabytes of data by 2025,"
 Apr. 2023. [Online]. Available: https://iotbusinessnews.com/2020/08/10/08984-connected-devices-will-generate-79-zettabytes-of-data-by-2025/
- [2] A. Zanella, N. Bui, A. Castellani, L. Vangelista, and M. Zorzi, "Internet of Things for smart cities," *IEEE Internet Things J.*, vol. 1, no. 1, pp. 22–32, Feb. 2014.
- [3] G. Ananthanarayanan, P. Bahl, P. Bodík, K. Chintalapudi, M. Philipose, L. Ravindranath, and S. Sinha, "Real-time video analytics: The killer App for edge computing," *Computer*, vol. 50, no. 10, pp. 58–67, Oct. 2017.
- [4] J. Wang, B. Amos, A. Das, P. Pillai, N. M. Sadeh, and M. Satyanarayanan, "A scalable and privacy-aware IoT service for live video analytics," in *Proc. ACM MMSys*, Jun. 2017, p. 38–49.
- [5] P. Mach and Z. Becvar, "Mobile edge computing: A survey on architecture and computation offloading," *IEEE Commun. Surv. Tut.*, vol. 19, no. 3, pp. 1628–1656, Mar. 2017.
- [6] N. Abbas, Y. Zhang, A. Taherkordi, and T. Skeie, "Mobile edge computing: A survey," *IEEE Internet Things J.*, vol. 5, no. 1, pp. 450– 465, Sep. 2018.
- [7] S. Bi, C. K. Ho, and R. Zhang, "Wireless powered communication: opportunities and challenges," *IEEE Commun. Mag.*, vol. 53, no. 4, pp. 117–125, 2015.
- [8] H. Ding, Y. Guo, X. Li, and Y. Fang, "Beef up the edge: Spectrum-aware placement of edge computing services for the internet of things," *IEEE Trans. Mobile Comput.*, vol. 18, no. 12, pp. 2783–2795, Nov. 2018.
- [9] M. Mozaffari, W. Saad, M. Bennis, Y.-H. Nam, and M. Debbah, "A tutorial on UAVs for wireless networks: Applications, challenges, and open problems," *IEEE Commun. Surv. Tut.*, vol. 21, no. 3, pp. 2334– 2360, Mar. 2019.
- [10] X. Zhang, H. Zhang, W. Du, K. Long, and A. Nallanathan, "IRS empowered UAV wireless communication with resource allocation, reflecting design and trajectory optimization," *IEEE Trans. Wireless Commun.*, vol. 21, no. 10, pp. 7867–7880, Apr. 2022.
- [11] K. Meng, Q. Wu, S. Ma, W. Chen, K. Wang, and J. Li, "Throughput maximization for UAV-enabled integrated periodic sensing and communication," *IEEE Trans. Wireless Commun.*, vol. 22, no. 1, pp. 671–687, Jan. 2022.
- [12] C. Zhan and Y. Zeng, "Energy minimization for cellular-connected UAV: From optimization to deep reinforcement learning," *IEEE Trans. Wireless Commun.*, vol. 21, no. 7, pp. 5541–5555, Jan. 2022.
- [13] Y. Yuan, L. Lei, T. X. Vu, S. Chatzinotas, S. Sun, and B. Ottersten, "Energy minimization in UAV-aided networks: Actor-critic learning for constrained scheduling optimization," *IEEE Trans. Veh. Technol.*, vol. 70, no. 5, pp. 5028–5042, Apr. 2021.
- [14] Z. Yu, Y. Gong, S. Gong, and Y. Guo, "Joint task offloading and resource allocation in UAV-enabled mobile edge computing," *IEEE Internet Things J.*, vol. 7, no. 4, pp. 3147–3159, Jan 2020.
- [15] C. Deng, X. Fang, and X. Wang, "UAV-enabled mobile edge computing for AI applications: Joint model decision, resource allocation and trajectory optimization," *IEEE Internet Things J.*, vol. 10, no. 7, pp. 5662–5675, Apr. 2022.

- [16] S. R. Sabuj, D. K. P. Asiedu, K.-J. Lee, and H.-S. Jo, "Delay optimization in mobile edge computing: Cognitive UAV-assisted eMBB and mMTC services," *IEEE Trans. Cogn. Commun. Netw.*, vol. 8, no. 2, pp. 1019–1033, Feb. 2022.
- [17] W. Zhou, L. Fan, F. Zhou, F. Li, X. Lei, W. Xu, and A. Nallanathan, "Priority-aware resource scheduling for UAV-mounted mobile edge computing networks," *IEEE Trans. Veh. Technol.*, vol. 72, no. 7, pp. 9682–9687, Jul. 2023.
- [18] X. Chen, Y. Bi, G. Han, D. Zhang, M. Liu, H. Shi, H. Zhao, and F. Li, "Distributed computation offloading and trajectory optimization in multi-UAV-enabled edge computing," *IEEE Internet Things J.*, vol. 9, no. 20, pp. 20096–20110, May 2022.
- [19] L. Yang, H. Yao, J. Wang, C. Jiang, A. Benslimane, and Y. Liu, "Multi-UAV-enabled load-balance mobile-edge computing for IoT networks," *IEEE Internet Things J.*, vol. 7, no. 8, pp. 6898–6908, Feb. 2020.
- [20] G. Zheng, C. Xu, M. Wen, and X. Zhao, "Service caching based aerial cooperative computing and resource allocation in multi-UAV enabled MEC systems," *IEEE Trans. Veh. Technol.*, vol. 71, no. 10, pp. 10934– 10947, Jun. 2022.
- [21] B. Dai, J. Niu, T. Ren, Z. Hu, and M. Atiquzzaman, "Towards energy-efficient scheduling of UAV and base station hybrid enabled mobile edge computing," *IEEE Trans. Veh. Technol.*, vol. 71, no. 1, pp. 915–930, Nov. 2021.
- [22] A. Asheralieva and D. Niyato, "Hierarchical game-theoretic and reinforcement learning framework for computational offloading in uav-enabled mobile edge computing networks with multiple service providers," *IEEE Internet Things J.*, vol. 6, no. 5, pp. 8753–8769, Jun. 2019.
- [23] N. Zhao, Z. Ye, Y. Pei, Y.-C. Liang, and D. Niyato, "Multi-agent deep reinforcement learning for task offloading in UAV-assisted mobile edge computing," *IEEE Trans. Wireless Commun.*, vol. 21, no. 9, pp. 6949– 6960, Mar. 2022.
- [24] J. Chen, X. Cao, P. Yang, M. Xiao, S. Ren, Z. Zhao, and D. O. Wu, "Deep reinforcement learning based resource allocation in multi-UAVaided MEC networks," *IEEE Trans. Wireless Commun.*, vol. 71, no. 1, pp. 296–309, Jan. 2022.
- [25] Y. Mao, C. You, J. Zhang, K. Huang, and K. B. Letaief, "A survey on mobile edge computing: The communication perspective," *IEEE Commun. Surv. Tut.*, vol. 19, no. 4, pp. 2322–2358, Aug. 2017.
- [26] Y. Zeng and R. Zhang, "Energy-efficient UAV communication with trajectory optimization," *IEEE Trans. Wireless Commun.*, vol. 16, no. 6, pp. 3747–3760, Mar. 2017.
- [27] S. Zhang, Y. Zeng, and R. Zhang, "Cellular-enabled UAV communication: A connectivity-constrained trajectory optimization perspective," *IEEE Trans. Wireless Commun.*, vol. 67, no. 3, pp. 2580–2604, Nov. 2018.
- [28] M. Li, N. Cheng, J. Gao, Y. Wang, L. Zhao, and X. Shen, "Energy-efficient UAV-assisted mobile edge computing: Resource allocation and trajectory optimization," *IEEE Trans. Veh. Technol.*, vol. 69, no. 3, pp. 3424–3438, Jan. 2020.
- [29] G. Yang, R. Dai, and Y.-C. Liang, "Energy-efficient UAV backscatter communication with joint trajectory design and resource optimization," *IEEE Trans. Wireless Commun.*, vol. 20, no. 2, pp. 926–941, Oct. 2020.
- [30] W. Wang, X. Li, R. Wang, K. Cumanan, W. Feng, Z. Ding, and O. A. Dobre, "Robust 3D-trajectory and time switching optimization for dual-UAV-enabled secure communications," *IEEE J. Sel. Areas Commun.*, vol. 39, no. 11, pp. 3334–3347, Jun. 2021.
- [31] M. Cui, G. Zhang, Q. Wu, and D. W. K. Ng, "Robust trajectory and transmit power design for secure UAV communications," *IEEE Trans. Veh. Technol.*, vol. 67, no. 9, pp. 9042–9046, Jun. 2018.
- [32] H. Lee, S. Eom, J. Park, and I. Lee, "UAV-aided secure communications with cooperative jamming," *IEEE Trans. Veh. Technol.*, vol. 67, no. 10, pp. 9385–9392, Jul. 2018.
- [33] X. Li, W. Feng, J. Wang, Y. Chen, N. Ge, and C.-X. Wang, "Enabling 5G on the ocean: A hybrid satellite-UAV-terrestrial network solution," *IEEE Wireless Commun.*, vol. 27, no. 6, pp. 116–121, Sep. 2020.
- [34] Y. Huang, W. Mei, J. Xu, L. Qiu, and R. Zhang, "Cognitive UAV communication via joint maneuver and power control," *IEEE Trans. Wireless Commun.*, vol. 67, no. 11, pp. 7872–7888, Jul. 2019.
- [35] F. Wang, J. Xu, X. Wang, and S. Cui, "Joint offloading and computing optimization in wireless powered mobile-edge computing systems," *IEEE Trans. Wireless Commun.*, vol. 17, no. 3, pp. 1784–1797, Dec. 2018.
- [36] Y. Xu, T. Zhang, Y. Liu, D. Yang, L. Xiao, and M. Tao, "UAV-assisted MEC networks with aerial and ground cooperation," *IEEE Trans. Wireless Commun.*, vol. 20, no. 12, pp. 7712–7727, Jun. 2021.

- [37] Y. Wang, M. Sheng, X. Wang, L. Wang, and J. Li, "Mobile-edge computing: Partial computation offloading using dynamic voltage scaling," *IEEE Trans. Wireless Commun.*, vol. 64, no. 10, pp. 4268–4282, Aug. 2016
- [38] G. Scutari, F. Facchinei, and L. Lampariello, "Parallel and distributed methods for constrained nonconvex optimization—part I: Theory," *IEEE Trans. Signal Process.*, vol. 65, no. 8, pp. 1929–1944, Dec. 2017.
- [39] S. P. Boyd and L. Vandenberghe, Convex optimization. Cambridge University Press, 2018.
- [40] T. Lipp and S. Boyd, "Variations and extension of the convex–concave procedure," *Optim. Eng.*, vol. 17, pp. 263–287, Jun. 2016.
- [41] W. Yuan and K. Nahrstedt, "Energy-efficient soft real-time CPU scheduling for mobile multimedia systems," AMC Symp. Oper. Syst. Principles (SOSP), vol. 37, no. 5, p. 149–163, Oct. 2003.
- [42] —, "Energy-efficient CPU scheduling for multimedia applications," *ACM Trans. Comput. Syst.*, vol. 24, no. 3, p. 292–331, Aug. 2006.
- [43] M. Grant and S. Boyd, "CVX: Matlab software for disciplined convex programming, version 2.1," http://cvxr.com/cvx, Mar. 2014.



Yu Zhang (S'19) received the B.Eng. degree in navigation technology from Wuhan University of Technology, Wuhan, China, in 2013, and the M.S. degree in information technology and management from University of Texas at Dallas, Dallas, Tx, USA, in 2017, respectively. He is pursuing the Ph.D. degree in electrical and computer engineering at University of Texas at San Antonio, San Antonio, TX, USA, where he works on resource management for satellite-terrestrial networks. He is a student member of IEEE.



Yanmin Gong (M'16, SM'21) received the B.Eng. degree in electronics and information engineering from Huazhong University of Science and Technology, Wuhan, China, in 2009, the M.S. degree in electrical engineering from Tsinghua University, Beijing, China, in 2012, and the Ph.D. degree in electrical and computer engineering from the University of Florida, Gainesville, FL, USA, in 2016. She is currently an Associate Professor of Electrical and Computer Engineering with The University of Texas at San Antonio, San Antonio, TX, USA. Her

research interests lie at the intersection of machine learning, cybersecurity, and networking systems. Dr. Gong is a recipient of the NSF CAREER Award, Cisco Research Award, the NSF CRII Award, the IEEE Computer Society TCSC Early Career Researchers Award for Excellence in Scalable Computing, the Rising Star in Networking and Communications Award by IEEE ComSoc N2Women, and the Best Paper Award at IEEE GLOBECOM. She has been serving on the editorial boards of ACM Computing Surveys, IEEE Transactions on Dependable and Secure Computing, and IEEE Wireless Communications.



Yuanxiong Guo (M'14, SM'20) received the B.Eng. degree in electronics and information engineering from the Huazhong University of Science and Technology, Wuhan, China, in 2009, and the M.S. and Ph.D. degrees in electrical and computer engineering from the University of Florida, Gainesville, FL USA, in 2012 and 2014, respectively. He is currently an Associate Professor in the Department of Information Systems and Cyber Security at the University of Texas at San Antonio, San Antonio, TX, USA. His current research interests include distributed

machine learning, applied data science, and trustworthy AI with application to digital health, energy sustainability, and human-robot collaboration. He is on the Editorial Board of IEEE Transactions on Vehicular Technology and servers as the track co-chair for IEEE VTC 2021-Fall. He is a recipient of the Best Paper Award in the IEEE GLBOECOM 2011.